

Cross-Correlated Motions in Azidolyszyme

Seyedeh Maryam Salehi and Markus Meuwly*

*Department of Chemistry, University of Basel, Klingelbergstrasse 80 , CH-4056 Basel,
Switzerland.*

E-mail: m.meuwly@unibas.ch

December 2, 2021

Abstract

The changes in the local and global dynamics of azide-labelled Lysozyme compared with that of the wild type protein are quantitatively assessed for all alanine residues along the polypeptide chain. Although attaching $-N_3$ to alanine residues has been considered to be a minimally invasive change in the protein it is found that depending on the location of the Alanine residue the local and global changes in the dynamics differ. For Ala92 the change in the cross correlated motions are minimal whereas attaching $-N_3$ to Ala90 leads to pronounced differences in the local and global correlations as quantified by cross correlation coefficients of the C_α atoms. It is also demonstrated that the spectral region of the asymmetric azide stretch distinguishes between alanine attachment sites whereas changes in the low frequency, far-infrared region are less characteristic.

Introduction

To characterize cellular processes at a molecular level the structure and dynamics of proteins needs to be understood. Such knowledge is also valuable to direct development and improvement of pharmaceutically active ligands in drug design efforts.¹⁻³ Optical spectroscopy is one possibility to capture the structural and functional dynamics of proteins in the condensed phase. One of the great challenges is to probe site-selective dynamics. This is required in order to specifically target protein sites that are responsible for function.

During the past 10 years a range of non-natural small molecule modifications to proteins has been proposed. They include - but are not limited to - attaching nitrile to amino acids,⁴ using the sulfhydryl band of cysteines,⁵ cyano⁶ groups, nitrile labels,⁷ complexation with SCN,⁸ cyanophenylalanine,⁹ or cyanamide.¹⁰ For Lysozyme, ruthenium carbonyl complexes have also been shown to provide an understanding of the water dynamics from 2d-infrared

experiments.¹¹⁻¹³ In this case it has been explicitly demonstrated that dynamic hydration extends over distances 20 Å away from the protein surface, consistent with recent simulations on hydrated Hb.^{14,15}

Based on recent studies¹⁶ the vibrational dynamics of N_3^- in the gas phase and in solution can be captured quantitatively.¹⁷ Moreover, azidoalanine (AlaN_3) is one of ideal labels that has been shown to be positionally sensitive probe for the local dynamics.¹⁶ AlaN_3 has a comparatively large extinction coefficient and it absorbs around $\sim 2100 \text{ cm}^{-1}$. The incorporation of N_3^- to alanine (Ala) is technically feasible and leads to small perturbations.¹⁸ Thus, AlaN_3 as also shown previously,¹⁶ is an ideal modification to study the local protein dynamics.

In the previous work, N_3^- was attached to all Ala residues in Lysozyme with the aim to determine changes in the local dynamics around the modification sites and effects on the global dynamics of the protein. First, the methods are discussed. Next, results on the root mean squared fluctuations and the dynamical cross correlation maps are presented. finally, the spectroscopy in the low-frequency and around the asymmetric azide stretch vibration is considered and conclusions are drawn.

Methods

Molecular Dynamics Simulation

Molecular Dynamics (MD) simulations of WT and all the modified AlaN_3 labels is done using CHARMM¹⁹ force field. For the simulations with multi-dimensional RKHS PES, an interface is written.¹⁷ MD simulations are performed with TIP3P water²⁰ model in a cubic box of size $(62.1)^3 \text{ Å}^3$. Figure 1 represents the Lysozyme structure used in the current

study with all modified Ala residues. The initial x-ray structure corresponds to WT human Lysozyme (3FE0²¹). First, the system is minimized followed by heating and equilibration for 100 ps. Then, the production runs of 2 ns are carried out for all 14 AlaN₃ labels using *NVT* ensemble and snapshots for analysis were recorded every 5 fs. Bond lengths involving H-atoms were constrained using the SHAKE²² algorithm and all non-bonded interactions were evaluated using shifted interactions with a cutoff of 14 Å switched at 10 Å.²³

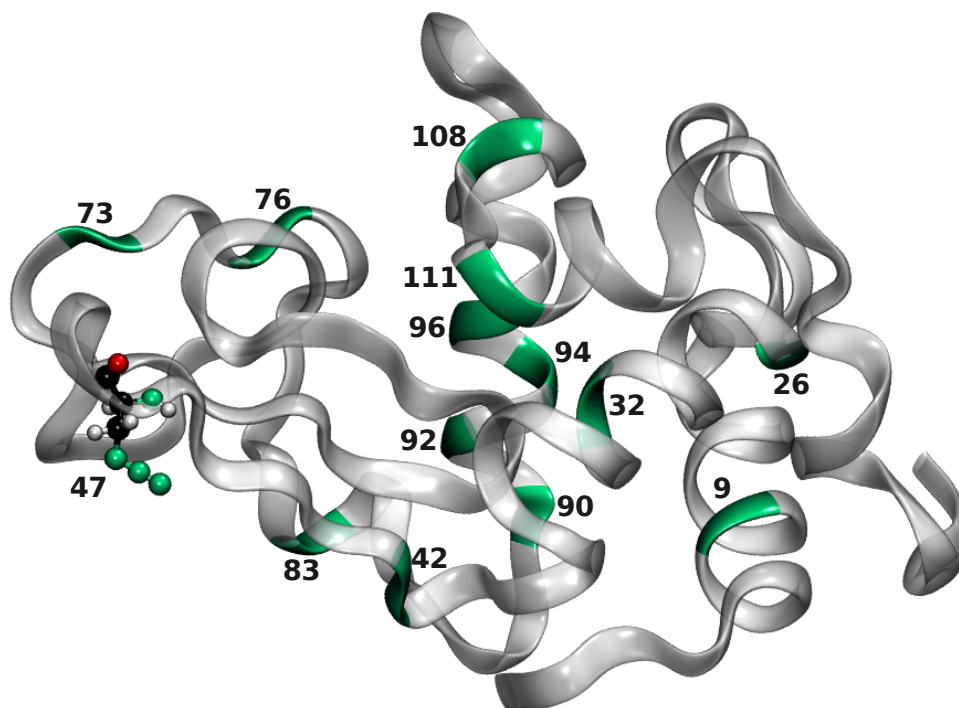


Figure 1: Lysozyme structure with indicated alanine residues at positions 9, 26, 32, 42, 47, 73, 76, 83, 90, 92, 94, 96, 108, 111. Ala residues are displayed as green NewRibbons while the rest of the protein structure is shown with white NewRibbons. Ala47N₃ is demonstrated in CPK as an example of alanine modified residue.

Dynamical Cross Correlation Maps

To quantitatively determine the effect of ligand binding on the protein dynamics, dynamical cross correlation maps^{24,25} (DCCM) and difference dynamical cross correlation maps

(Δ DCCM) are calculated using the Bio3D package.²⁶ Dynamic cross-correlation matrices with coefficients

$$C_{ij} = \langle \Delta r_i \cdot \Delta r_j \rangle / (\langle \Delta r_i^2 \rangle \langle \Delta r_j^2 \rangle)^{1/2} \quad (1)$$

were determined from the positions of the main chain C_α atoms in amino acids i and j with positions r_i and r_j . Δr_i and Δr_j determine the displacement of the i th C_α from its mean position over the entire trajectory. For DCCM calculation, the Bio3D package²⁶ is used. Note that DCCMs describes the correlated and anti-correlated motions in a protein whereas differences Δ DCCM report on pronounced differences between unmodified and modified proteins.

Infrared Spectroscopy

The infrared spectrum is calculated by the Fourier transform over the dipole moment autocorrelation function. To that end, the dipole moment $\vec{\mu}$ is obtained for the entire protein and $-N_3$ label separately from the simulation trajectories of 2 ns production run. For the IR spectra the correlation function $C(t) = \langle \vec{\mu}(0) \vec{\mu}(t) \rangle$ was determined from snapshots saved every 5 fs. Then, the fast Fourier transform of $C(t)$ was determined using a Blackman filter and the result was multiplied using a quantum correction factor $\beta \hbar \omega / (1 - \exp(-\beta \hbar \omega))$ where $\beta = 1/(k_B T)$.²⁷

Results

Global Dynamics (RMSF and DCCM)

To probe the flexibility or rigidity of the unmodified and modified proteins the root mean squared fluctuation (RMSF) of lysozyme in solution before and after modification is compared with original X-ray structure as the reference. The comparison is based on all C_α atoms in the protein and the result is shown in Figure 2 for all Ala residues. The RMSF

changes of the modified proteins compared with unmodified Lysozyme range from minor (Ala26, Ala32, Ala42, Ala73, Ala76, Ala92, Ala96, Ala108, Ala111) to major (Ala9, Ala47, Ala83, Ala90, Ala94), see Figure 2. Moreover, attaching an $-N_3$ label to one site may also lead to larger fluctuations at other neighbor or non-neighbor residues. As an example, modification of Ala47 to Ala47 N_3 leads to larger RMSFs for residues 12 to 18, 45 to 49, 87 to 93, and 122 to 130.

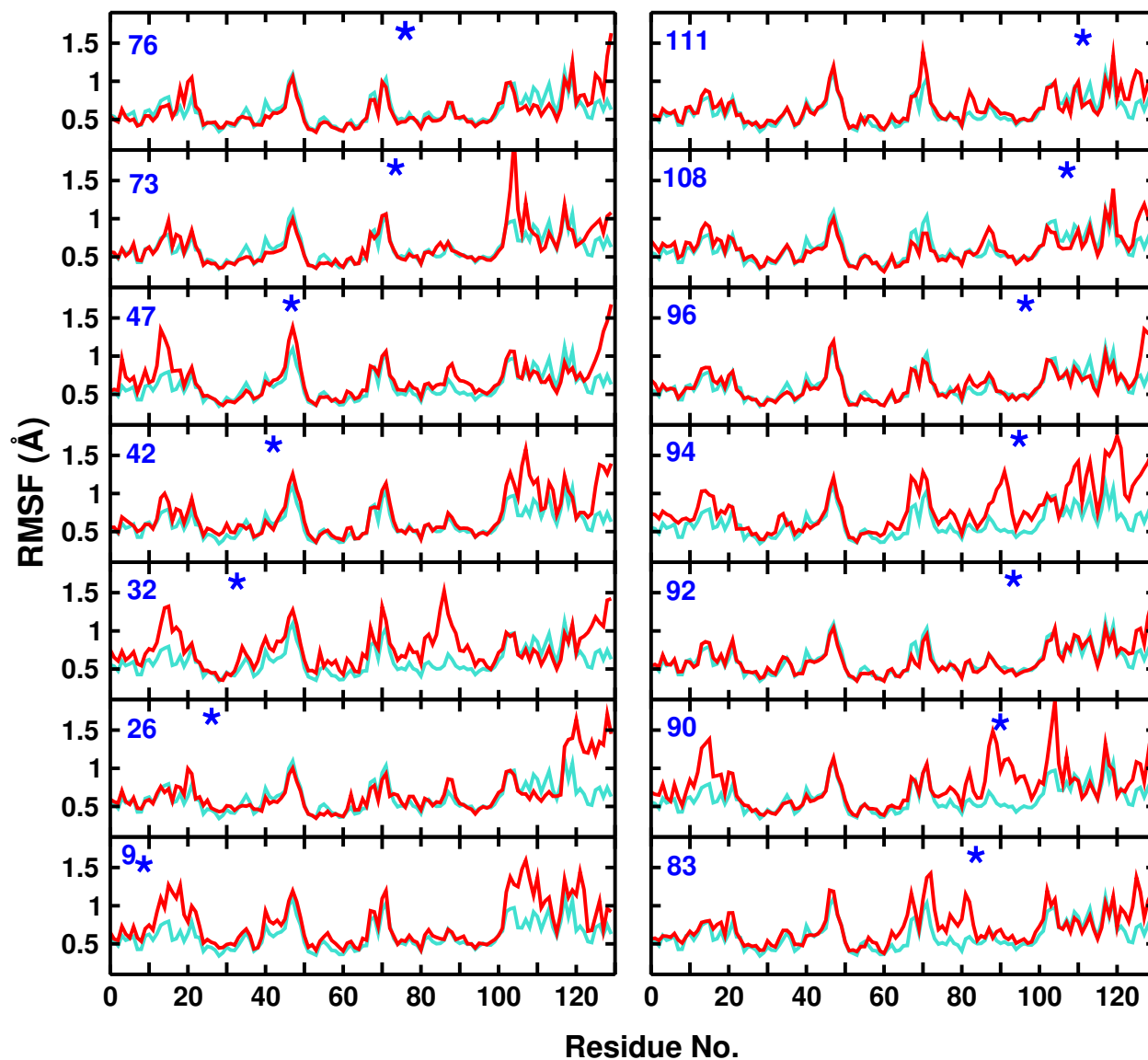


Figure 2: Root mean squared fluctuations for the C_{α} atoms of the WT (turquoise) protein and including different AlaN_3 (red) modification sites. The position of the modified residue is indicated by an asterisk.

Another example for a more pronounced change in the local flexibility concerns modification of Ala32. In this case the region for residues 80 to 100 becomes considerably more flexible which can also be explained by the close contact of the two helices Ala32 on the one hand and residues 90 to 100 are part of, see Figure 1. Finally, attaching N_3 to Ala94 leads to a range of changes in the flexibility of nearby and more distant residues, including residues [10-20], [60-70], [85-100], and [110-130]. It is noteworthy to remark that in general, attaching

-N₃ leads to increased flexibility of the protein and that often the terminus around residue 130 becomes more flexible. One example for which the flexibility is decreased concerns modification at Ala108 for which the region [65-75] becomes more rigid.

Dynamical Cross Correlation Maps: DCCMs describe the correlated ($C_{ij} \sim 1$) and anti-correlated ($C_{ij} \sim -1$) motions within a protein. As an example, the DCCMs for the WT lysozyme and Ala108N₃ are shown in Figure 3. Bulges along the diagonal correspond to helices whereas features extending away from the diagonal orthogonal to it are β -sheet structures. For the WT there is a hinge motion at the intersection between residues 10 and 50 with $0.25 \leq C_{ij} \leq 0.5$ which disappears upon modification at position Ala108. The intensity of such hinge motions should be compared with insulin monomer for which disulfide bonds are characterized by $0.55 \leq C_{ij} \leq 0.70$, i.e. about a factor of two more intense than in the present case. Similarly, there are several anticorrelated motions in the WT protein, e.g. involving residues 10 and 80 or 50 and 110 which largely disappear upon modification at Ala108. It is also instructive to compare the DCCM with the RMSF in Figure 2. As was already discussed, the RMSF for Ala108N₃ is reduced for residues in the range [65,75] compared with the WT protein. This can also be seen in the DCCM for which the positive correlation involving residues [70-80,60] is considerably stronger in the WT compared with the modified protein.

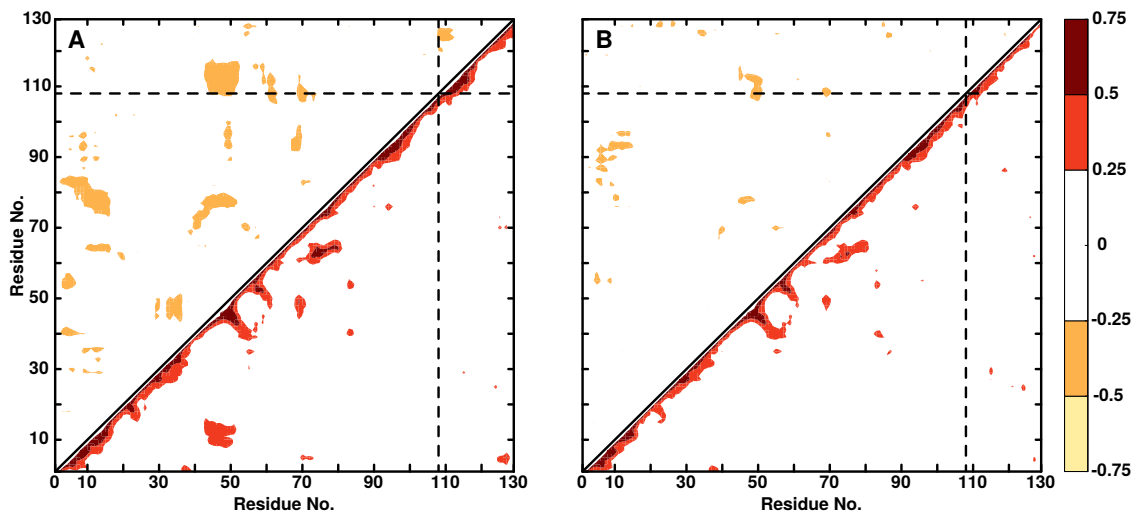


Figure 3: DCCM for WT lysozyme (panel A) and Ala108N₃ (panel B). Positive correlations are in the lower right triangle, negative correlations in the upper left triangle. Only correlation coefficients with an absolute value greater than 0.25 are displayed.

Local dynamics (Δ DCCM)

To further analyze the modification sites, difference maps Δ DCCM are calculated for all the AlaN₃ modifications which report on residues with pronounced changes in the dynamics after modification. The range of differences considered includes changes ($> |0.25|$) and smaller than ($> |0.75|$). For differences $|\Delta C_{ij}| < 0.25$ the changes are too insignificant whereas values $|\Delta C_{ij}| > 0.75$ were not observed.

Figure 4 shows the corresponding Δ DCCM maps for residues Ala92N₃, Ala26N₃, and Ala90N₃ as examples for minor, medium and major effects on the protein dynamics after modification. Incorporation of -N₃ into the protein at position Ala92 leads to insignificant changes in the correlation between the residues (Figure 4 top panel). This is consistent with the findings from analysis of the RMSF, see Figure 2, which shows only minor variation in the fluctuations without and with N₃ attached to Ala92. On the contrary, for Ala26N₃ ligand-induced effects between residues [12, 18] and [42, 52] (feature A) and residues [23, 35] and [120, 127] (feature B) are found, see Figure 4 middle panel. Again, these changes can also be found

in the RMSF analysis in Figure 2 although there, the effects specifically for residues [12,18] and [23,35] are smaller, albeit still visible. Both, local (feature B) and global (feature A) changes in the protein dynamics are found.

Finally, the difference map for Ala90N₃ (Figure 4 bottom panel) shows strong effects on the dynamics and couplings between residues after attaching N₃ to the Alanine residue. Feature A indicates coupling between residues [90, 102] and [5, 18]/[85, 90]/[113, 128] whereas feature B refers to coupled residues [3, 18] and [87, 89]/[27 – 38]. It is noted that residues [5, 18] and [87, 89] are common between feature A and B. These findings suggest that residues couple both locally and through space. Again, residues involved in features A and B belong to those with the largest variations in the RMSF, see Figure 2. For other Δ DCCM representations, see Figure S1 to S10.

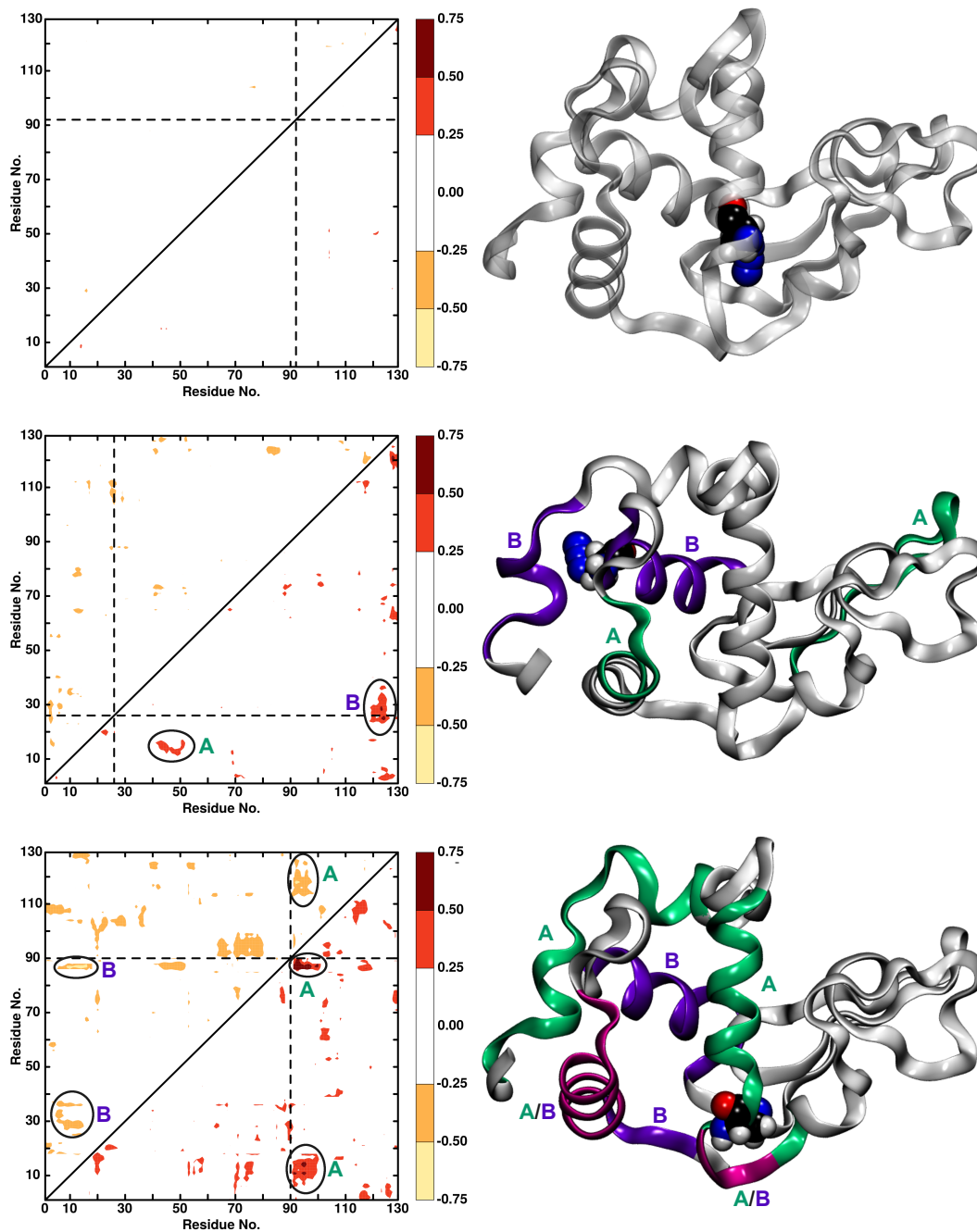


Figure 4: Difference dynamic cross correlation maps (Δ DCCM) between WT and Ala92N₃, Ala26N₃, Ala90N₃ (top to bottom). Positive differences are in the lower right triangle, negative differences in the upper left triangle. Only differences with an absolute value greater than 0.25 are displayed. Right panels show the protein structure with features A (green) and B (violet) and common residues between feature A and B (magenta) of Δ DCCM plots highlighted in color. The AlaN₃ label is shown in VDW.

Spectroscopy

It is also of interest to further consider the vibrational spectroscopy for the different modified proteins. In particular, it is of interest whether attaching the azide label at different positions along the polypeptide chain leads to discernible changes only in the asymmetric N_3 stretch vibration or whether the spectroscopy in the low-frequency (far infrared, THz) range is also expected to be affected by the modification.

Figure 5A reports the IR spectrum in the low frequency range ($0-300\text{ cm}^{-1}$) with modifications at positions 9, 47, and 73 together with the high frequency range ($2130-2230\text{ cm}^{-1}$, panel B) which captures the asymmetric stretch of the $-N_3$ label. The IR spectrum for all $AlaN_3$ modifications is shown in Figure S11. Using the same energy function for all $AlaN_3$ moieties, the results demonstrate that the IR spectra differ in terms of the position of the frequency maxima and their full widths at half maximum (FWHM). Compared with earlier work which determined the 1-d IR lineshape from the frequency fluctuation correlation function (FFCF)¹⁶ the present analysis confirms that the frequency maxima of the most red (Ala9) and most blue (Ala73) shifted azide vibrations differ by $\sim 15\text{ cm}^{-1}$.

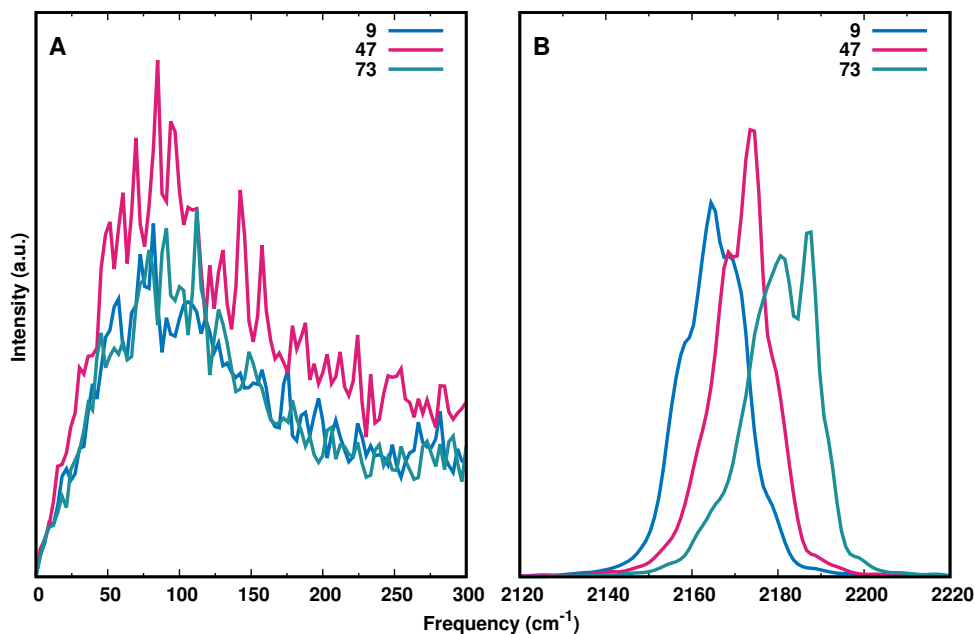


Figure 5: IR spectrum from Fourier Transform of the dipole moment auto-correlation function of the entire protein (panel A) and the $-N_3$ label (panel B) for $AlaN_3$ modifications at positions 9 (blue), 47 (red), and 73 (green). The results show that the region around the asymmetric N_3 stretching vibration is considerably more discriminating than the THz region of the spectrum.

In addition, the spectrum in the low-frequency region (0 to 300 cm^{-1}) is reported in Figure 5A. The FFCFs determined previously reported pronounced oscillations for $-N_3$ -modification at Ala9, Ala32, Ala42, and Ala92 but their origin remains unclear. Similarly, earlier work in the region of the antisymmetric stretch of the N_3^- anion in ternary complexes with formic acid dehydrogenase and NAD^+ and $NADH$, respectively, also reported oscillations on the picosecond time scale of the FFCF.²⁸ Importantly, in this earlier work the azide anion is not covalently bound to either the protein or the ligand but rather replaces the formate reactant as a transition state analogue in the active site of the protein. The reported oscillations occur on the sub-picosecond to picosecond time scale. For the covalently bound azide label the recurrences are rather on the sub-ps time scale throughout. It was hypothesized that these recurrences potentially originate from coupling of the azide label to low frequency modes of the environment. However, the spectra in Figure 5A do not support such an interpretation

as irrespective of the position of the azide label the spectral signatures in the range between 0 and 300 cm^{-1} are largely identical.

Conclusion

The results discussed here confirm that azide attached to protein alanine residues provides site-specific information about the spectroscopy and dynamics. This is consistent with earlier findings for Lysozyme and PDZ2..^{16,29} Changes in difference dynamical cross correlation maps range from insignificant to major in that attaching $-\text{N}_3$ to Ala90 leads to major changes in the overall protein dynamics through altered couplings across the entire protein. On the other hand, this pronounced change in the protein dynamics is not necessarily reflected in the infrared spectroscopy of the azide label. Finally, it is demonstrated that the spectral region of the asymmetric azide stretch discriminates much more than the far infrared region which does not appear to exhibit specific features depending on the location of the modification site. The present work provides a molecularly resolved view of the internal protein dynamics upon introducing small spectroscopic probes at strategic positions of a protein.

Acknowledgments

The authors gratefully acknowledge financial support from the Swiss National Science Foundation through grant 200021-117810 and to the NCCR-MUST.

Data Availability Statement

The data that support the findings of this study are available from the corresponding author upon reasonable request.

References

- (1) Plitzko, J. M.; Schuler, B.; Selenko, P. Structural Biology outside the box - inside the cell. *Curr. Op. Struct. Biol.* **2017**, *46*, 110–121.
- (2) Guo, J.; Zhou, H.-X. Protein Allostery and Conformational Dynamics. *Chem. Rev.* **2016**, *116*, 6503–6515.
- (3) Lu, S.; He, X.; Ni, D.; Zhang, J. Allosteric Modulator Discovery: From Serendipity to Structure-Based Design. *J. Med. Chem.* **2019**, *62*, 6405–6421.
- (4) Getahun, Z.; Huang, C.; Wang, T.; De Leon, B.; DeGrado, W.; Gai, F. Using nitrile-derivatized amino acids as infrared probes of local environment. *J. Am. Chem. Soc.* **2003**, *125*, 405–411.
- (5) Kozinski, M.; Garrett-Roe, S.; Hamm, P. 2D-IR spectroscopy of the sulfhydryl band of cysteines in the hydrophobic core of proteins. *J. Phys. Chem. B* **2008**, *112*, 7645–7650.
- (6) Zimmermann, J.; Thielges, M. C.; Seo, Y. J.; Dawson, P. E.; Romesberg, F. E. Cyano Groups as Probes of Protein Microenvironments and Dynamics. *Angew. Chem. Int. Ed.* **2011**, *50*, 8333–8337.
- (7) Bagchi, S.; Boxer, S. G.; Fayer, M. D. Ribonuclease S Dynamics Measured Using a Nitrile Label with 2D IR Vibrational Echo Spectroscopy. *J. Phys. Chem. B* **2012**, *116*, 4034–4042.
- (8) van Wilderen, L. J. G. W.; Kern-Michler, D.; Mueller-Werkmeister, H. M.; Bredenbeck, J. Vibrational dynamics and solvatochromism of the label SCN in various solvents

- and hemoglobin by time dependent IR and 2D-IR spectroscopy. *Phys. Chem. Chem. Phys.* **2014**, *16*, 19643–19653.
- (9) Horness, R. E.; Basom, E. J.; Thielges, M. C. Site-selective characterization of Src homology 3 domain molecular recognition with cyanophenylalanine infrared probes. *Anal. Chem.* **2015**, *7*, 7234–7241.
- (10) Lee, G.; Kossowska, D.; Lim, J.; Kim, S.; Han, H.; Kwak, K.; Cho, M. Cyanamide as an Infrared Reporter: Comparison of Vibrational Properties between Nitriles Bonded to N and C Atoms. *J. Phys. Chem. B* **2018**, *122*, 4035–4044.
- (11) King, J. T.; Kubarych, K. J. Site-specific coupling of hydration water and protein flexibility studied in solution with ultrafast 2D-IR spectroscopy. *J. Am. Chem. Soc.* **2012**, *134*, 18705–18712.
- (12) King, J. T.; Arthur, E. J.; Brooks III, C. L.; Kubarych, K. J. Site-specific hydration dynamics of globular proteins and the role of constrained water in solvent exchange with amphiphilic cosolvents. *J. Phys. Chem. B* **2012**, *116*, 5604–5611.
- (13) King, J. T.; Arthur, E. J.; Brooks, C. L., III; Kubarych, K. J. Crowding Induced Collective Hydration of Biological Macromolecules over Extended Distances. *J. Am. Chem. Soc.* **2014**, *136*, 188–194.
- (14) El Hage, K.; Hedin, F.; Gupta, P. K.; Meuwly, M.; Karplus, M. Valid molecular dynamics simulations of human hemoglobin require a surprisingly large box size. *Elife* **2018**, *7*, e35560.
- (15) Pezzella, M.; El Hage, K.; Niesen, M. J.; Shin, S.; Willard, A. P.; Meuwly, M.; Karplus, M. Water dynamics around proteins: T-and R-States of hemoglobin and melittin. *J. Phys. Chem. B* **2020**, *124*, 6540–6554.

- (16) Salehi, S. M.; Meuwly, M. Site-selective dynamics of azidolysosome. *J. Chem. Phys.* **2021**, *154*.
- (17) Salehi, S. M.; Koner, D.; Meuwly, M. Vibrational Spectroscopy of N_3^- in the Gas and Condensed Phase. *J. Phys. Chem. B* **2019**, *123*, 3282–3290.
- (18) Kiick, K.; Saxon, E.; Tirrell, D.; Bertozzi, C. Incorporation of azides into recombinant proteins for chemoselective modification by the Staudinger ligation. *Proc. Natl. Acad. Sci.* **2002**, *99*, 19–24.
- (19) MacKerell, A. D.; Bashford, D.; Bellott, M.; Dunbrack, R. L.; Evanseck, J. D.; Field, M. J.; Fischer, S.; Gao, J.; Guo, H.; Ha, S. et al. All-atom Empirical Potential for Molecular Modeling and Dynamics Studies of Proteins. *J. Phys. Chem. B* **1998**, *102*, 3586–3616.
- (20) Jorgensen, W. L.; Chandrasekhar, J.; Madura, J. D.; Impey, R. W.; Klein, M. L. Comparison of Simple Potential Functions for Simulating Liquid Water. *J. Chem. Phys.* **1983**, *79*, 926–935.
- (21) Chiba-Kamoshida, K.; Matsui, T.; Ostermann, A.; Chatake, T.; Ohhara, T.; Tanaka, I.; Yutani, K.; Niimura, N. X-ray crystal structure of wild type human lysozyme in D_2O . DOI: 10.2210/pdb3fe0/pdb.
- (22) Gunsteren, W. V.; Berendsen, H. Algorithms for Macromolecular Dynamics and Constraint Dynamics. *Mol. Phys.* **1997**, *34*, 1311–1327.
- (23) Steinbach, P. J.; Brooks, B. R. New Spherical-Cutoff Methods for Long-Range Forces in Macromolecular Simulation. *J. Comput. Chem.* **1994**, *15*, 667–683.
- (24) Ichiye, T.; Karplus, M. Collective Motions in Proteins - A Covariance Analysis of Atomic Fluctuation in Molecular-Dynamics and Normal Mode Simulations. *Protein Struct. Funct. Genet.* **1991**, *11*, 205–217.

- (25) Arnold, G.; Ornstein, R. Molecular dynamics study of time-correlated protein domain motions and molecular flexibility: Cytochrome P450BM-3. *Biophys. J.* **1997**, *73*, 1147–1159.
- (26) Grant, B. J.; Rodrigues, A. P. C.; ElSawy, K. M.; McCammon, J. A.; Caves, L. S. D. Bio3d: an R package for the comparative analysis of protein structures. *Bioinformatics* **2006**, *22*, 2695–2696.
- (27) Schmitz, M.; Tavan, P. Vibrational spectra from atomic fluctuations in dynamics simulations. II. Solvent-induced frequency fluctuations at femtosecond time resolution. *J. Chem. Phys.* **2004**, *121*, 12247–12258.
- (28) Pagano, P.; Guo, Q.; Kohen, A.; Cheatum, C. M. Oscillatory enzyme dynamics revealed by two-dimensional infrared spectroscopy. *J. Phys. Chem. Lett.* **2016**, *7*, 2507–2511.
- (29) Zanobini, C.; Bozovic, O.; Jankovic, B.; Koziol, K. L.; Johnson, P. J. M.; Hamm, P.; Gulzar, A.; Wolf, S.; Stock, G. Azidohomoalanine: A Minimally Invasive, Versatile, and Sensitive Infrared Label in Proteins To Study Ligand Binding. *J. Phys. Chem. B* **2018**, *122*, 10118–10125.

Supporting Information: Cross-Correlated Motions in Azidolyszyme

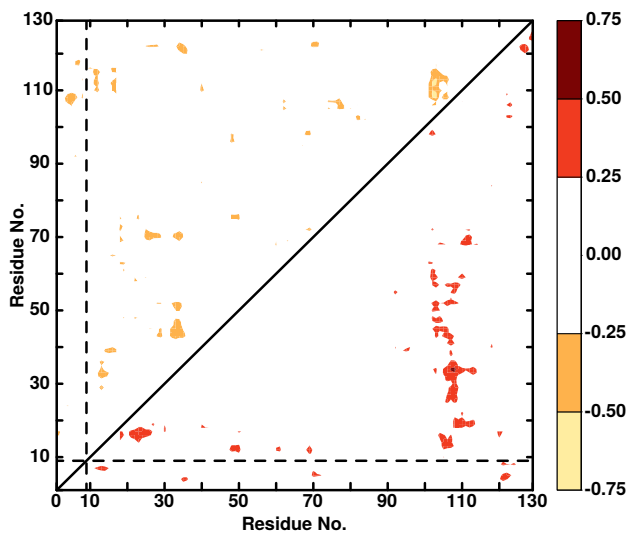


Figure S1: Δ DCCM between WT and Ala9N₃. Positive differences are in the lower right triangle, negative differences in the upper left triangle. Only differences with an absolute value greater than 0.25 are displayed.

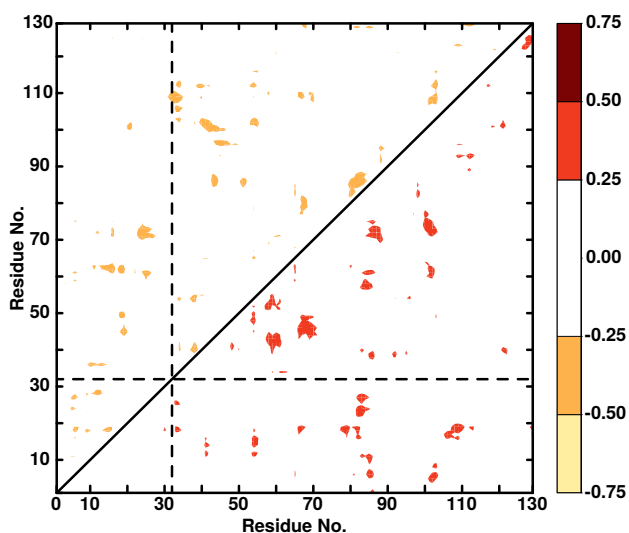


Figure S2: Δ DCCM between WT and Ala32N₃. Positive differences are in the lower right triangle, negative differences in the upper left triangle. Only differences with an absolute value greater than 0.25 are displayed.

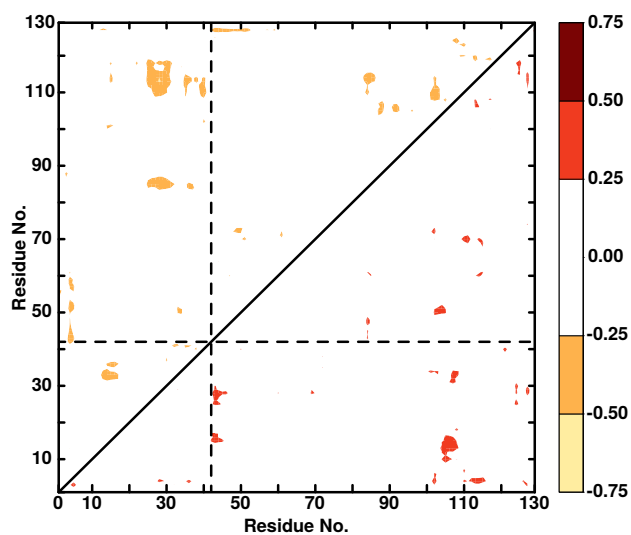


Figure S3: Δ DCCM between WT and Ala42N₃. Positive differences are in the lower right triangle, negative differences in the upper left triangle. Only differences with an absolute value greater than 0.25 are displayed.

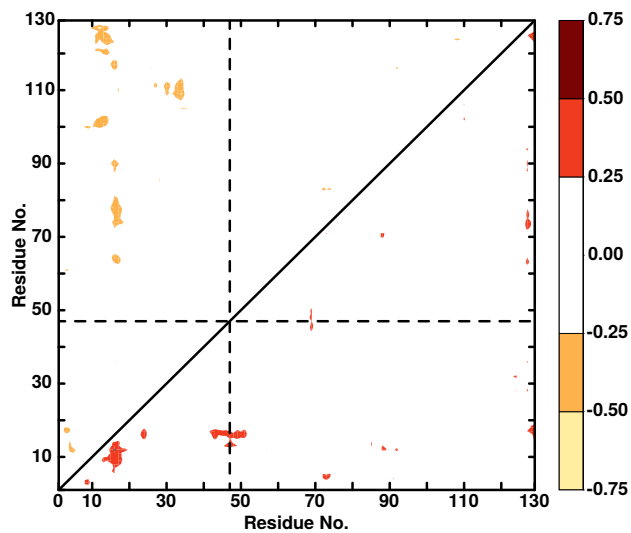


Figure S4: Δ DCCM between WT and Ala47N₃. Positive differences are in the lower right triangle, negative differences in the upper left triangle. Only differences with an absolute value greater than 0.25 are displayed.

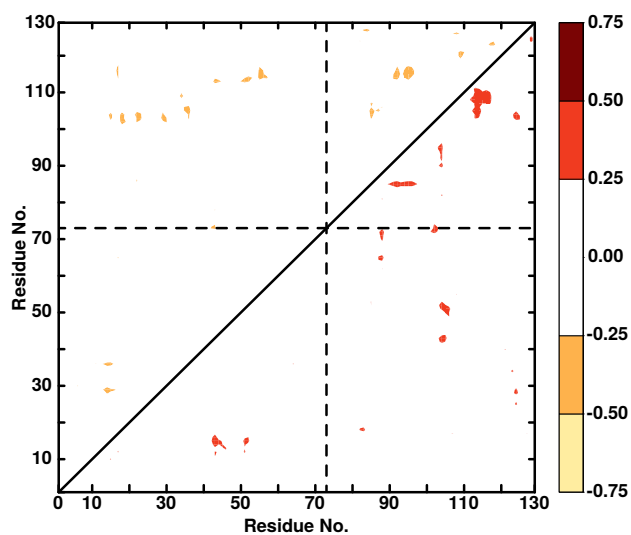


Figure S5: Δ DCCM between WT and Ala73N₃. Positive differences are in the lower right triangle, negative differences in the upper left triangle. Only differences with an absolute value greater than 0.25 are displayed.

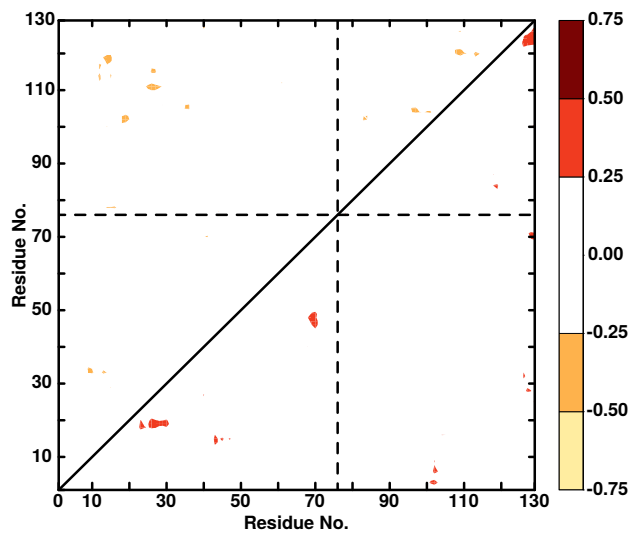


Figure S6: Δ DCCM between WT and Ala76N₃. Positive differences are in the lower right triangle, negative differences in the upper left triangle. Only differences with an absolute value greater than 0.25 are displayed.

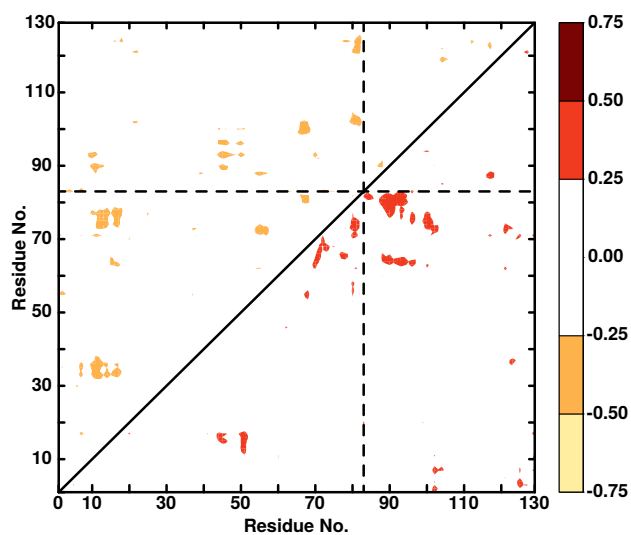


Figure S7: Δ DCCM between WT and Ala83N₃. Positive differences are in the lower right triangle, negative differences in the upper left triangle. Only differences with an absolute value greater than 0.25 are displayed.

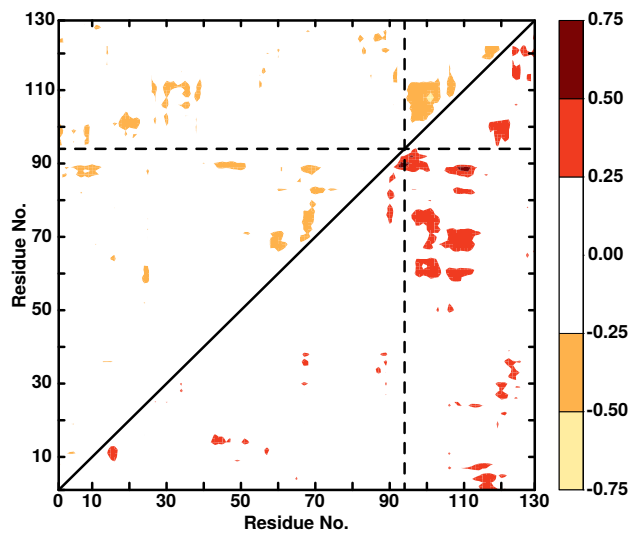


Figure S8: Δ DCCM between WT and Ala94N₃. Positive differences are in the lower right triangle, negative differences in the upper left triangle. Only differences with an absolute value greater than 0.25 are displayed.

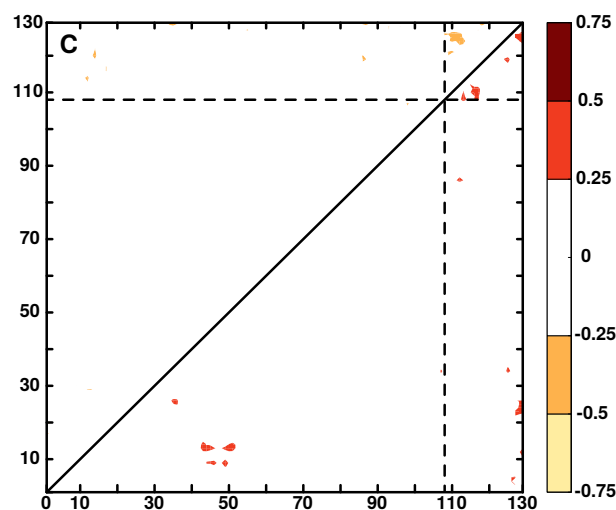


Figure S9: Δ DCCM between WT and Ala108N₃. Positive differences are in the lower right triangle, negative differences in the upper left triangle. Only differences with an absolute value greater than 0.25 are displayed.

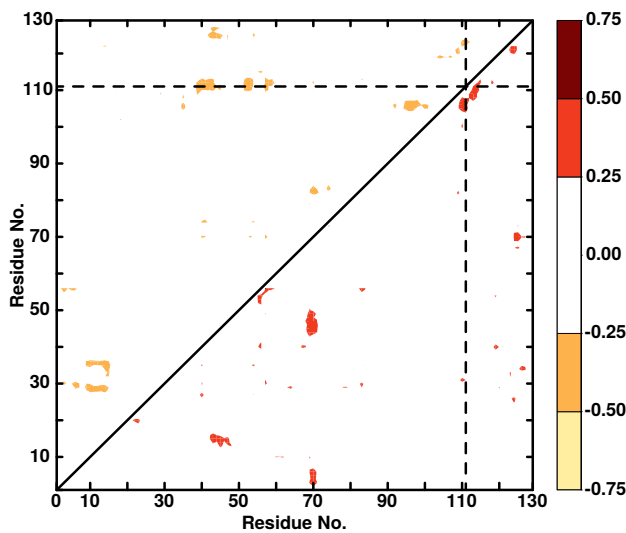


Figure S10: Δ DCCM between WT and Ala111N₃. Positive differences are in the lower right triangle, negative differences in the upper left triangle. Only differences with an absolute value greater than 0.25 are displayed.

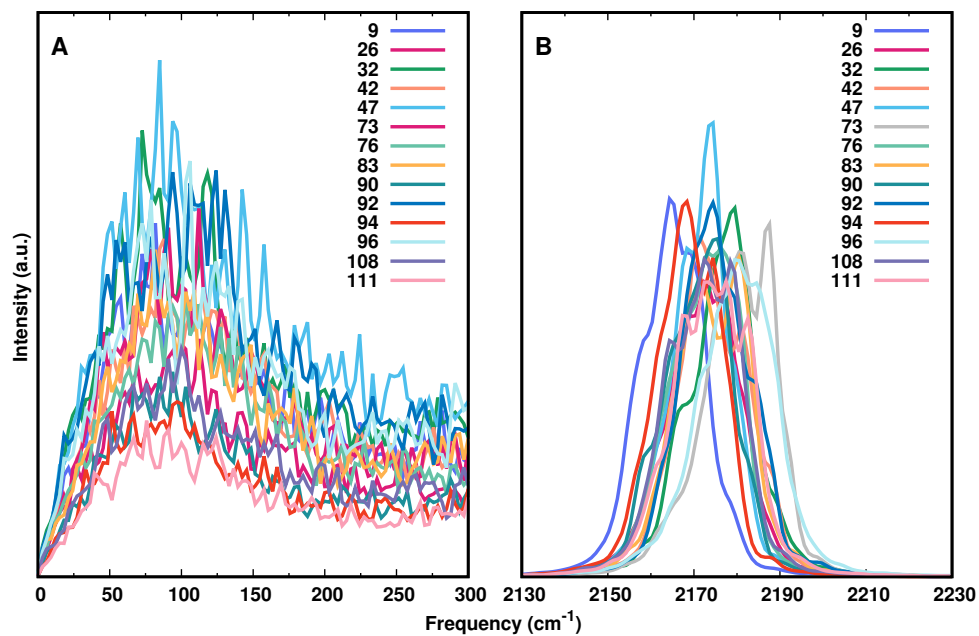


Figure S11: IR spectrum obtained from Fourier Transform of the dipole moment auto-correlation function of protein (panel A) and -N₃ label (panel B) for all AlaN₃ modifications. The labels in each panel refer to the alanine residue that carries the -N₃ moiety.